Engineering 14 (2022) 181–191

Contents lists available at ScienceDirect

Engineering

journal homepage: www.elsevier.com/locate/eng

Research
Passive Intermodulation Measurement—Review

Passive Intermodulation Measurement: Challenges and Solutions

Zhanghua Cai [a,b], Lie Liu [a,*], Francesco de Paulis [c], Yihong Qi [a,b,*]

[a] General Test Systems Inc., Shenzhen 518000, China
[b] College of Electrical and Information Engineering, Hunan University, Changsha 410082, China
[c] UAq EMC Laboratory, Department of Industrial and Information Engineering and Economics, University of L'Aquila, L'Aquila 64100, Italy

ARTICLE INFO

Article history:
Received 21 August 2021
Revised 5 January 2022
Accepted 28 February 2022
Available online 20 April 2022

Keywords:
Passive intermodulation (PIM)
PIM source location
Anechoic chamber

ABSTRACT

In modern wireless communication systems, the signal-to-noise ratio (SNR) is one of the most important performance indicators. When the other radio frequency (RF) performance of the components is well designed, passive intermodulation (PIM) interference may become an important factor limiting the system's SNR. Whether it is a base station, an indoor distributed antenna system, or a satellite system, there are stringent PIM level requirements to minimize interference and enhance network capacity in multicarrier networks. Especially for systems of high power and wide bandwidth such as 5G wireless communication, PIM interference is even more serious. Due to the complexity and uncertainty of PIM, measurement is the most important means to study and evaluate the PIM performance of wireless communication systems. In this review, the current main PIM measurement methods recommended by International Electrotechnical Commission (IEC) and other standard organizations are introduced, and several key challenges in PIM measurement and their solutions (including the design of PIM tester, the location of the PIM sources, the design of compact PIM anechoic chambers, and the evaluation methods of PIM anechoic chambers) are highlighted. These challenges are of great significance to solve PIM problems that may arise during device characterization and verification in real wireless communication systems.

1. Introduction

The signal-to-noise ratio (SNR) is the most significant figure of merit in communication systems for ensuring reliable receiver functionalities. The reduction of noise and interference is what all radio scientists and engineers have devoted their consistent effort to. The interferences generated in passive components at the system front end are one of the most serious concerns. The nonlinear interference problem of passive devices, components, and systems is called passive intermodulation (PIM) [1,2]. PIM is one of the important factors limiting the SNR of the system. When two or more signals exist in a nonlinear component, mixed signals composed of the original frequencies could be generated. In the case that the frequency of the mixed signals is within the passband of the receiver, PIM interference occurs. When the PIM level is higher than the noise floor of the system, it can significantly reduce the SNR at the receiver. For systems that have both receiving and transmitting functions, the PIM products generated by high-power signals in the transmitting path may directly enter and affect the receiving path. In this case, PIM has a particularly obvious impact on the SNR. Taking a base station as an example [3], a typical PIM level of −104.9 dBm is very close to the noise floor of −103 dBm in the Universal Terrestrial Radio Access (UTRA) carrier. A slightly higher PIM level may severely increase the noise floor. As the SNR decreases by 1 dB, the channel capacity will decrease by about 11% [4], thus greatly affecting system performances. In satellite communications, the impact of PIM is even more serious since the PIM level is usually required to be around −200 dBc. To achieve better performances of the radio communication link, various PIM indicators must be analyzed, measured, and controlled through design, manufacturing process, and even after installation in the base station. Moreover, the current trend in the development of communication systems driven by ever-changing technologies and requirements, such as 5G wireless systems, intelligent connected vehicles, high-power, and multi-band or wideband specifications, will inherently lead to more PIM problems.

* Corresponding authors.
E-mail addresses: lie.liu@generaltest.com (L. Liu), yihong.qi@generaltest.com (Y. Qi).

https://doi.org/10.1016/j.eng.2022.02.012

The sources of PIM can typically be divided into two types: contact nonlinearity and material nonlinearity. The first cause refers to current flowing through any type of junction between different materials that generates a nonlinear behavior. It mainly includes two types of contacts, namely, metal–metal and metal–insulator–metal type of contacts. Also, loose oxidized or contaminated metallic joints falls in this category. The second cause is material nonlinearity, which refers to material characterized by a nonlinear current response due to an applied voltage. This type of behavior may be associated to conductive, dielectric, or magnetic properties of materials [5].

The physical mechanisms that cause nonlinear responses are complex and diverse [6]. Some examples are provided below: electron tunneling semiconductor effect [7–9]; micro-discharge between the voids in metal–metal interface [10–12]; electro–thermal effect [13–15]; contact resistance effect [16–18]; and ferromagnetic effect [19–21].

The mechanisms listed above may also be combined so that the final PIM effect can be attributed to two or more sources. As an example, there may be nonlinearities caused by tunneling, ferromagnetic effects, contact resistance, and so forth, on the coaxial connector at the same time. Moreover, new materials, new structures, and complex integration technologies may all bring new PIM interference effects due to the combination and interaction of the above mechanisms.

Hence, it is very important to conduct theoretical analysis on the possible PIM sources when developing a new technology or device. Recently, many researchers have adopted modeling and simulation methods to analyze the PIM of typical devices. Henrie et al. [22,23] proposed a PIM model applied to coaxial connectors, which can predict the PIM of coaxial connectors in microwave networks. Furthermore, Guo et al. [24] proposed a generalized PIM network model with multiple connectors. Jin et al. [25,26] carried out modeling and analysis on the influence of the coating material in connectors and the iron content in the base brass. The mechanism of PIM in printed lines was discussed in Refs. [27–31], and a series of PIM models of distributed nonlinear transmission lines were proposed, which can provide some guidance on reducing PIM. The PIM at waveguide flanges was studied in Refs. [16,17,32]. A full-wave frequency domain method was used to evaluate the PIM of reflector antennas in Refs. [33,34]. Figueiredo et al. [35] proposed a novel nonlinear system characterization method that can be used as a guideline for system design, modeling, and compensation.

The above analysis methods can provide practical guidelines for reducing PIM. The methods to reduce PIM can be roughly summarized into three categories. The first one aims at changing the design of the device to avoid or reduce PIM. For example, the gap waveguide is used to achieve contactless flange connections in Ref. [36], which can greatly reduce the PIM level of the waveguide. According to the analysis in Ref. [28], the PIM of printed lines can be reduced by adding geometrical discontinuities. The second is applied to the devices whose design cannot be changed; in such cases, the PIM level can be lowered by improving the manufacturing process by minimizing the loose parts, by better smoothing any burr, or by selecting the materials to be assembled having similar conductivity. For example, better coating materials can be selected [25,26]. The third solution involves a system-level PIM signal cancellation [23,37–41]. For example, Henrie et al. [23,37] cancelled the original PIM by adding a known nonlinear interposer network, which can effectively reduce the PIM without the special design of nonlinear devices. Waheed et al. [38] proposed a digital cancellation solution to suppress PIM in the system, and they demonstrated a PIM suppression of more than 20 dB. This method can effectively alleviate the requirements for device linearity [38].

However, most of the above-mentioned analysis methods are developed for specific devices. For actual systems, multiple PIM sources and multiple mechanisms coexist, which may require a combination of multiple analysis methods and solutions. In this way, the complexity of theoretical analysis will increase, and the accuracy in the prediction of the improved PIM will decrease. Therefore, it is also practically important to identify the PIM sources by experimental tests and thus to evaluate the device performance by a final system-level measurement. The standardized PIM measurement process is well described in the International Electrotechnical Commission (IEC) Standard IEC62037 [42]. However, some relevant aspects and challenges when making practical PIM measurements are not mentioned therein. These aspects are of great importance for the accuracy of the PIM measurement and for the identification of the PIM sources. The relevant PIM interference problems are listed below, and these challenges are mainly related to the measurements of the mixing products generated by lumped nonlinearities.

The first challenge is the design of the PIM tester with a large dynamic range and wide working bandwidth. The PIM test instrument is the prerequisite for making any PIM measurement. The main challenge of the PIM tester is to detect relatively low PIM values within a large frequency bandwidth. Generally, the PIM noise floor of the measurement system needs to be 5–10 dB lower than the PIM level of the device under test (DUT) in order to obtain accurate measurement results [42]. Therefore, for mobile communication systems, the PIM noise floor is usually required to be lower than −170 dBc. The satellite communication system has higher requirements, with a needed noise floor of nearly −200 dBc. This requires the very high performance of the devices within the measurement system. The PIM performances of power amplifiers, filters, couplers, and other core components determine the performance of the overall system. In addition, various signal cancellation techniques can also be used in PIM testers, which can effectively improve the dynamic range of the system [43–45].

The second important challenge is accurately locating the PIM source. The theoretical analysis will inevitably miss some PIM sources especially for complex systems with multiple PIM sources, and it is usually not effective in the evaluation of the magnitude of PIM. The level of the PIM depends on the degree of nonlinearity and the magnitude of the current passing through the nonlinear node. The nonlinearity is difficult to evaluate in many cases, such as rust on the metal surface or loose joints and the amount of ferromagnetic material in the metal; thus, controlling the current is the key to reducing the PIM. However, in the design of microwave components such as antennas, usually only global parameters such as voltage standing wave ratio (VSWR) and gain are concerned, with the magnitude of the current being only rarely analyzed. Also, it is difficult to determine which PIM sources have a significant impact on the system. Some PIM source identification methods have been reported for different types of devices in Refs. [46–59]. For example, the near-field scanning measurement method can be used to detect non-closed PIM sources such as printed lines [49–52]. Acoustic vibration is used to detect PIM sources in base station antennas [53]. The method based on a *k*-space multicarrier signal can be used to locate multiple PIM sources in microwave systems [54].

The following two challenges are related to the PIM test chamber. Anechoic chamber plays an important role in improving the accuracy of PIM measurement. These are the work done by some of the authors.

The third challenge is to design a compact chamber with low background PIM. The PIM interference largely depends on the processing and assembly of each piece of the chamber. The PIM level will change with small changes in the structure, such as different surface roughness of the conductor, thin oxide layer or surface

contamination, loose contact, and debris in the contact area. Different samples of the same product may be characterized by different PIM performances. Therefore, production line measurement should be done for products with strict PIM requirements. In addition, the PIM performance may be changed during long-distance transportation due to loose connectors and surface contamination. Therefore, on-site PIM measurement after the chamber installation is also very important to ensure that the PIM specifications of the equipment are always within the allowable range. The traditional large-size chamber is expensive and covers a large estate. A low-PIM anechoic chamber design method is proposed in Ref. [60], which can be used to realize a miniaturized, low-cost, and high-precision PIM test chamber. It can be used as a solution for production lines or on-site PIM measurements.

The fourth challenge is the evaluation method of the PIM chamber. Usually, the manufacturer will give the background PIM noise of the chamber. This is sufficient for non-radiating components, but it may not be appropriate for radiating components. The structure of the chamber itself also generates PIM signals, and the harmonic power depends on the energy radiated to the chamber PIM source. For example, assume that there are two antennas with different gains, and their real PIM values are both −150 dBc. During the measurement, the energy radiated by the low-gain antenna is small, and the possible interference is only −160 dBc, which hardly affects the results. However, the high-gain antenna may produce −150 dBc or even greater PIM interference, which will cause large errors in the measurement. Therefore, the evaluation of the chamber should be related to the gain of the DUT. A method for evaluating the PIM level of the chamber using a low-PIM medium-gain antenna is proposed in Ref. [61]. By reducing the path loss, this method equates a medium-gain antenna to a high-gain antenna, avoiding the difficulty of designing a high-gain and low-PIM antenna.

The rest of this review is arranged as follows. The characteristics of PIM interference is introduced in Section 2. In Section 3, the basic PIM measurement methods will be reviewed according to the international standard IEC62037. The challenges and solutions of PIM measurement will be elaborated in Section 4. Finally, the full paper is summarized.

2. Characteristics of PIM interference

In order to understand PIM, the basic theory of the harmonics and intermodulation products should be known. The nonlinear function of the passive device can be characterized by the following power series (the direct current (DC) term is omitted):

$$y = \sum_{k=1}^{\infty} a_k x^k \tag{1}$$

where x and y represent instantaneous input and output signals, respectively; the coefficient a_k is related to the nonlinear characteristics of the device (k is the order of the power series). When the input signal is a single-frequency signal with frequency f_1, harmonic signals that are integer multiples of the fundamental frequency will appear in the output signal according to Eq. (1), such as $2f_1$, $3f_1$, and so forth. As the harmonic order increases, the amplitude of the harmonic will generally decrease. Although there are some applications that use harmonics (e.g., harmonic mixers), harmonics in passive devices are usually undesired signals [62].

When the input signal is composed of two frequencies (f_1 and f_2), according to Eq. (1), there will be not only harmonic signals in the output signal but also intermodulation signals as the result of the combination of these two frequencies. The frequency of these signals can be collectively expressed as $mf_1 + nf_2$, where $|m| + |n|$ is called the order of the PIM signal.

Fig. 1 shows the intermodulation signal around the fundamental frequency. In most cases, the third-order PIM products are the most concerned unless high-order PIM interference should be considered for satellite communication systems. Most of the required PIM measurements are focused on the third-order PIM products since they are the closest to the operating frequency of the system, and usually their amplitude is the largest among all other odd-order products.

3. Standards on PIM measurement methods

Although the Third Generation Partnership Project (3GPP) and International Telecommunication Union (ITU) have released standards on PIM measurement [3,63], the details and guidelines on the measurement setup are not given. The PIM distortion test methods usually refer to the international standard IEC62037 [42]. The IEC62037 standard provides general requirements and methods for measuring the PIM noise of passive radio frequency (RF) and microwave devices. The standard defines the basic PIM test method, specifies the test power (43 dBm), and provides error analysis. At present, the principles of PIM test equipment and test methods in the industry are generally consistent with the standard.

The transmission and reflection methods are the basic PIM measurement methods provided by IEC Standard. Fig. 2 shows the typical measurement method of forward and reverse PIM at the same time. The terms reverse and forward are related to the direction of the measured PIM with respect to the nominal direction of the high-power signal. When measuring reverse PIM, the PIM signal generated by the DUT is reflected to Port 1 and detected by the spectrum analyzer (SA). When measuring the forward PIM, the PIM transmitted in the forward direction enters the SA from Port 2. When the DUT has two or more ports, the forward PIM measurement may be more commonly used, since this mode can usually reflect the worst case of the DUT. However, in the case of DUT with only one port such as antennas, the reverse PIM measurement method is easier to implement.

Extra components may be needed to measure the forward PIM of radiating DUTs such as antennas. Since the radiation system has only a single port, the forward PIM cannot be measured directly by applying the transmission method. The radiation method should be applied [64]. The principle is to radiate the generated PIM signal to the space through the DUT. The radiated PIM signal can be received by a probe antenna and detected by the SA for its analysis.

Although the IEC Standard describes the basic measurement methods, it cannot solve some important measurement problems. As mentioned above, the location of the PIM source is very important to be able to identify and solve any PIM problem. Thus, the standard method described in Fig. 2 cannot be of general applicability. In addition, for radiating DUTs, the control of environmental interference is the key aspect to improve the measurement

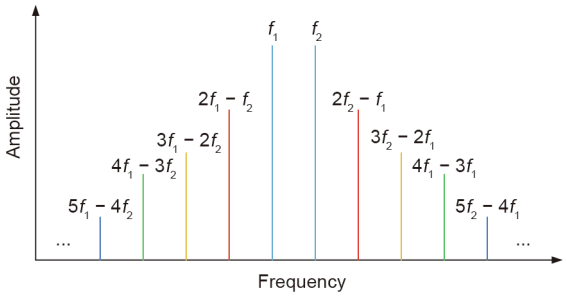

Fig. 1. PIM signal spectrum around the fundamental frequencies.

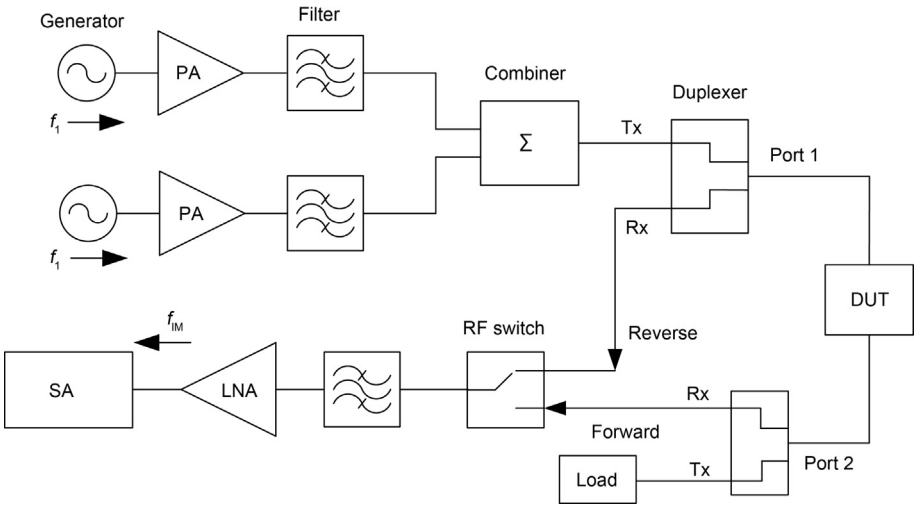

Fig. 2. Schematic map of PIM tester. PA: power amplifier; ∑: the symbol of combiner; Tx: transmit; Rx: receive; LNA: low noise amplifier; f_{IM}: frequency of the PIM signal; SA: spectrum analyzer.

accuracy, and this is usually achieved by performing the test inside anechoic chambers. The current standard does not accurately and specifically define the requirements for the measurement environment (anechoic chamber). The only specific requirement is that the absorption rate of the absorber is greater than 30 dB. This is far from being enough for the complete definition of the environmental requirements and suitable testing methods to be applied for their evaluation of anechoic chamber to be used for testing radiating DUTs. Moreover, the measurement setup and guidelines included in the current standards cannot meet the growing requirements due to the development of new devices. Therefore, the second part of this paper aims at reviewing the specific challenges posed by these important measurement problems and the corresponding proposed solutions.

4. Challenges and solutions of PIM measurement

4.1. Challenge and solution to design PIM tester

The PIM tester is the basis of PIM measurement. The PIM level of the electronic components determines the overall performance of the PIM tester. At present, manufacturers usually guarantee the performance of devices through strict screening, the use of expensive materials, and the improvement of manufacturing processes. There are also some research works aimed at improving the performance of the device through the unique design of signal synthesizers [65], filters [66], loads [67], and so forth.

In addition to improving the device itself, the use of feed-forward cancellation technology is also an effective method to improve system performance [43–45]. Feed-forward cancellation is a technique that generates a signal with the same amplitude and reverses phase as the original signal and then can cancel the original signal by summing. This method can only eliminate the interference caused by the feed-forward signal without affecting the PIM signal generated by the DUT. Therefore, the feed-forward cancellation technology is particularly suitable for eliminating interference in PIM measurement systems. As shown in Fig. 3 [43], the high dynamic range PIM measurement system is mainly composed of signal sources, amplifiers, isolators, combiners, and so forth, as proposed in Ref. [43]. The system only needs to detect the power of the signal and the combined power of the detection and cancellation signal to predict the phase shift required for cancellation, and can adaptively eliminate the interference signal in the feed-forward signal. This technology can extend the dynamic range of the system by at least 40 dB within a broadband, and can achieve a dynamic range of 113 dB in a two-tone test system. The power spectral density can be improved significantly according to the difference of transport with and without cancellation. Such digital cancellation method is especially useful for 5G carrier aggregation, which is designed to meet the demands for higher data rates.

4.2. Challenge and solution to locate PIM source

The identification of the PIM source plays an important role in solving PIM interference. There are mainly two traditional methods for locating PIM sources. One is the tapping test, which uses a small rubber hammer or screwdriver handle to tap each possible PIM source positions in the network while continuously monitoring the PIM level. Under this type of interference, defective components will cause large fluctuations in the PIM level. The second one is the segmentation elimination method; it is based on disassembling the entire network and measuring part of the components to gradually narrow down the possible locations of PIM sources and finally determine the components that generate the PIM. However, the above methods all require manual action, it is time-consuming and labor-intensive, and it may not accurately locate the PIM source. Many researchers have studied this problem, among which the typical identification methods are described.

At present, some PIM analyzers have integrated PIM source positioning functions, such as Kaelus [46], Rosenberger [47], Anritsu [48], among others. The core of its fault location technology is to adopt the principle of time domain reflectometer (TDR). The reflected PIM signal sweeps a certain frequency range. The time domain pulse can be reconstructed using inverse fast Fourier transform (IFFT) on the reflected signal. This kind of PIM source location technology has many limitations. For example, in the actual antenna feeder system, the filter will bring extra time delay and reduce the positioning accuracy. In addition, the existence of multiple branches of the system will lead to positioning uncertainties.

The near-field scanning measurement is another typical method. The block diagram of the near-field measurement method is illustrated in Fig. 4 [50], as described in Refs. [27,49–52]. The basic principle is to use various probes (such as monopoles and small loop antennas) to make non-contact PIM measurements near

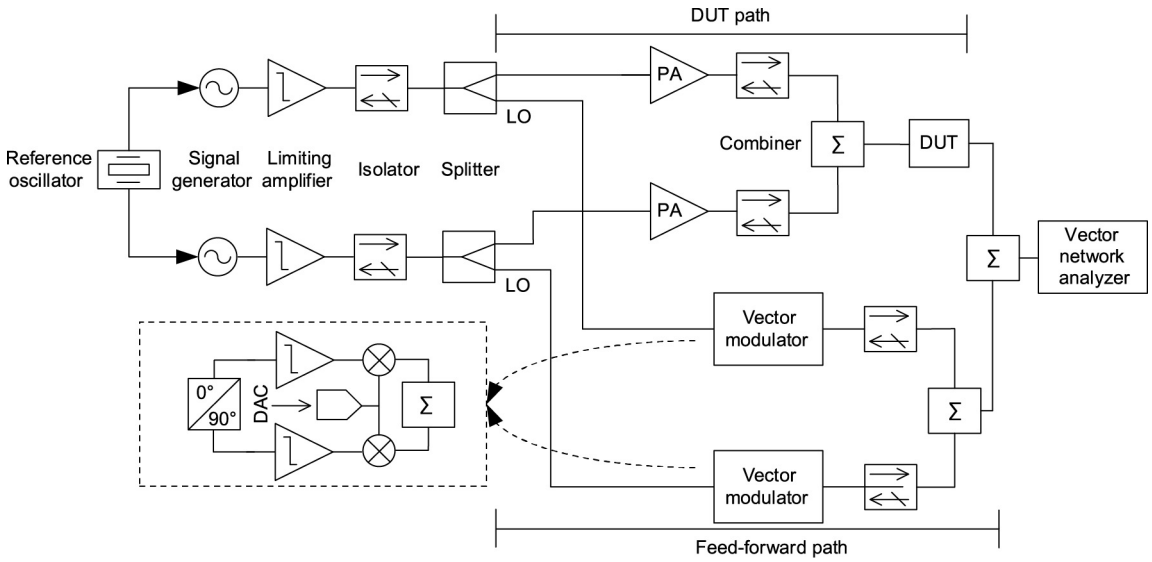

Fig. 3. High dynamic range PIM measurement system (a large value, low-PIM attenuator or coupler can be added at the output of the DUT to match the power of the vector network analyzer) [43]. LO: local oscillator; DAC: digital-to-analog converter.

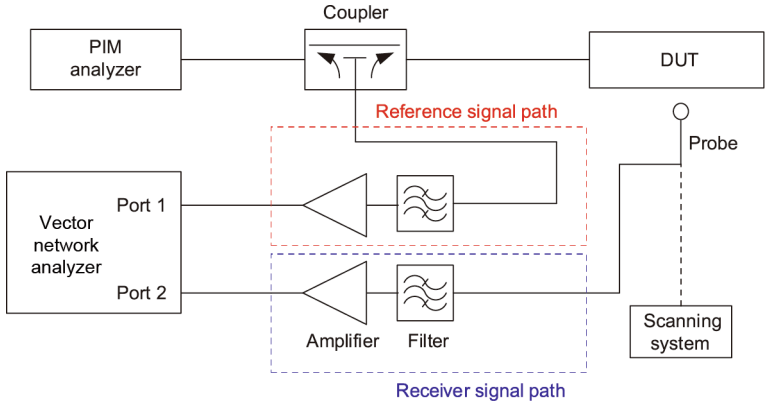

Fig. 4. Block diagram of the near-field measurement system [50].

the DUT. The position where the probe detects the maximum PIM signal field strength is, most probably, the location of the PIM source. Although the probe itself may be the source of PIM, the probe and the whole PIM test setup can be calibrated before the DUT testing in order to remove the weak nonlinearity introduced by the probe. This objective can be achieved by a differential measurement or by post processing the test results. This method was originally used to determine the location of the interference sources in base station antennas [49,50]. More recently, it has been used for the PIM measurement of printed circuits [27,51,52]. This method is a powerful tool for locating PIM sources of open structures, such as printed circuits. However, it cannot detect PIM sources inside enclosed components such as cables, waveguides, and cavity filters. PIM levels below −110 dBm can be detected in this method [50]. When used to locate the PIM source in a printed line, the accuracy of less than one centimeter can be achieved.

Due to the limitation found in the above PIM source location methods, a measurement method using acoustic vibration to locate the PIM source is proposed in Ref. [53]. Its principal block diagram is displayed in Fig. 5 [53]. The method is to introduce acoustic vibrations at different positions of DUT, and then identify the location of the PIM source by detecting the strength of the modulated PIM signal. The basic idea of this method is similar to the traditional tap test, but it is more systematic and more accurate. This method has been tested by engineering and has solved many PIM problems for base station manufacturers. Therefore, it can be considered as a relatively mature and effective PIM source location method. The accuracy of this method is about one centimeter. This method requires that the PIM source must be caused by loose mechanical contacts or loose nonlinear materials. In addition, for metal devices such as duplexers, the acoustic wave could propagate throughout the whole device. Therefore, the exact location of the PIM source in the duplexer cannot be accurately located.

Neither the near-field measurement nor the acoustic vibration method can locate multiple PIM sources at the same time. A multi-point positioning method based on coherent measurement technology is proposed in Ref. [54]. The block diagram is illustrated in Fig. 6 [54]. This method introduces a reference source into the PIM test system, and it uses the amplitude and phase difference between the reference source and the actual PIM sources to construct a *k*-space multicarrier signal. Based on the *k*-space inverse Fourier transform and inverse optimization of the multicarrier signal, a PIM localization algorithm is proposed. This method can be used to locate the position of multi-point PIM sources, which is suitable for both open and closed structures. The localization uncertainty of this method is proportional to the multiplication of the total DC phase error and the used bandwidth. This method is able to identify the distance between each PIM source and the

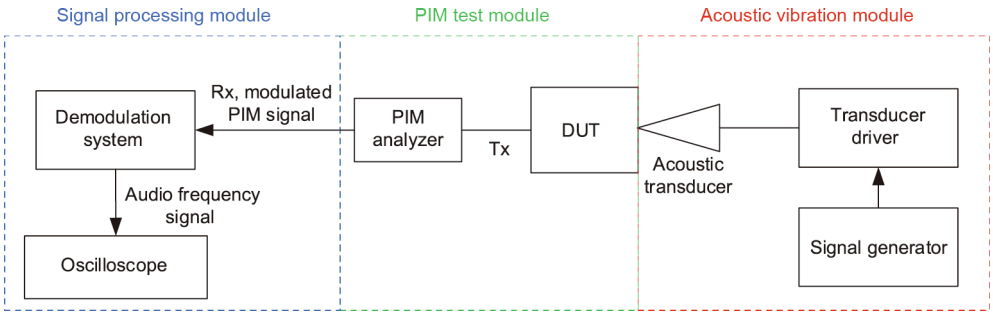

Fig. 5. Block diagram of a vibration modulation test system setup [53].

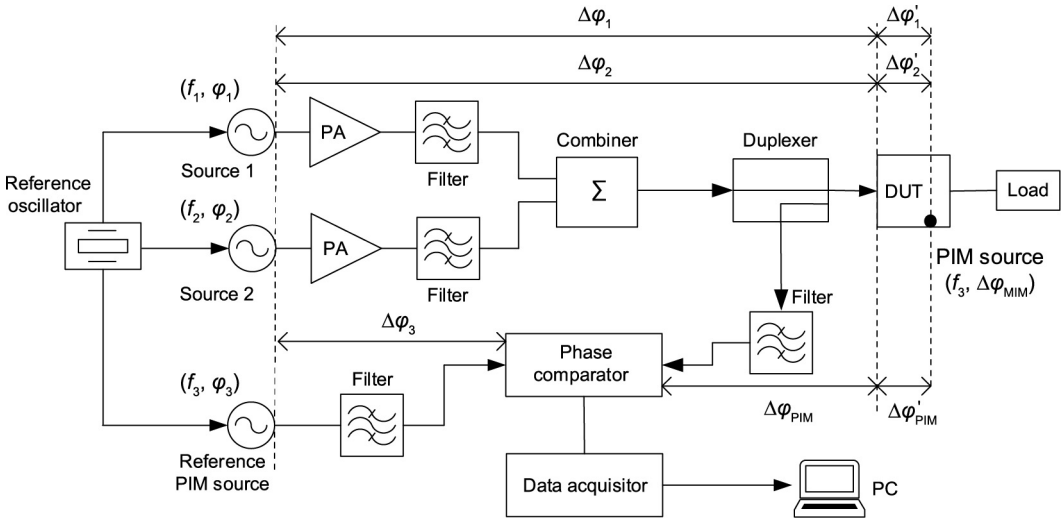

Fig. 6. Block diagram of a localization method based on the *k*-space multicarrier signal [54]. φ_1, φ_2, φ_3: the initial phase of the source f_1, f_2, and f_3, respectively; $\Delta\varphi_1$, $\Delta\varphi_2$: the phase delay between the output ports of the source f_1, f_2 and the input port of the DUT, respectively; $\Delta\varphi_3$: the phase delay between the output ports of the source f_3 and the phase comparator; $\Delta\varphi'_1$, $\Delta\varphi'_2$: the phase delay of the sources between the input port of the DUT and the location of the PIM source; $\Delta\varphi_{PIM}$: the phase delay of the PIM signal between the input port of the DUT and the comparator; $\Delta\varphi'_{PIM}$: the phase delay of the PIM signal between the PIM source and the input port of the DUT; $\Delta\varphi_{MIM}$: the potential inherent phase shift caused by the PIM source; PC: personal computer.

input port. However, for DUTs with multiple branches, uncertainty occurs in the localization of the branch in which the PIM source is occurring.

In addition to the above methods, some other PIM source location methods have been proposed. Aspden et al. [55–57] proposed the method of microwave holographic imaging to locate the PIM sources of reflector antennas. This method is to transmit two single-frequency signals to the reflector under test through low-PIM antennas. Then, a planar scanner is used to detect the amplitude and phase of the reflected wave on a two-dimensional plane. After data analysis, the coordinates of the PIM sources on the reflecting surface can be obtained. Yong et al. [58] proposed a method of using emission source microscopy (ESM) to locate PIM sources. ESM is a technique aimed at locating and characterizing interference sources by measuring the amplitude and phase of the field on a plane a few wavelengths away from the DUT [68–70]. The algorithm is based on the synthetic aperture radar technology, and on the two-dimensional Fourier transform. The field on the plane to be measured can be calculated from the field measured on the scanning plane. The measurement setup is shown in Fig. 7 [58]. This method does not need to feed the DUT and can identify the PIM source at a relatively large distance. Chen et al. [59] proposed a miniaturized waveguide cell with water filling. The block diagram is described in Fig. 8 [59]. The printed circuit board (PCB) only needs to be inserted into the waveguide twice to locate the PIM sources on the PCB. In this case, there is no need to feed the DUT. Thus, it is especially suitable for PCBs or other open planar structures that cannot be directly fed.

These methods are mainly devoted to PIM products generated by lumped nonlinearities, and usually for some obvious dominant nonlinearities, such as "rusty bolts." In the case of multiple PIM sources within close range, it may be difficult to accurately distinguish the sources, but at least people can know which component generated the PIM [50,53]. Due to the diversity of PIM sources, it is difficult to use one method to fulfill the PIM identification of all type of devices. Certain test methods are usually more effective for a specific type of devices. Therefore, the feasibility of these methods must be left to engineering inspection for the identification of the most suitable technique for the specific device to be tested.

4.3. Challenge and solution to design compact PIM test chamber

The PIM evaluation of radiating systems poses additional constraints when designing test chambers. In the case of radiating systems, the DUT can not only radiate energy into space but also receive energy from space. Therefore, the following interference sources may appear when measuring PIM: The RF signal radiated from the DUT may cause nearby objects to produce and re-radiate PIM signals; then, such PIM signals may be received by the DUT. The PIM signal radiated by the DUT may be received again due to the reflection of objects such as walls. Also, other RF signals

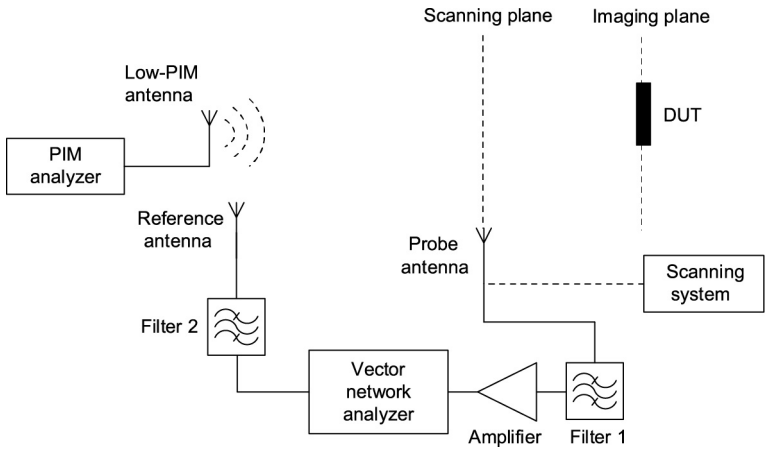

Fig. 7. Block diagram of a localization method based on ESM [58].

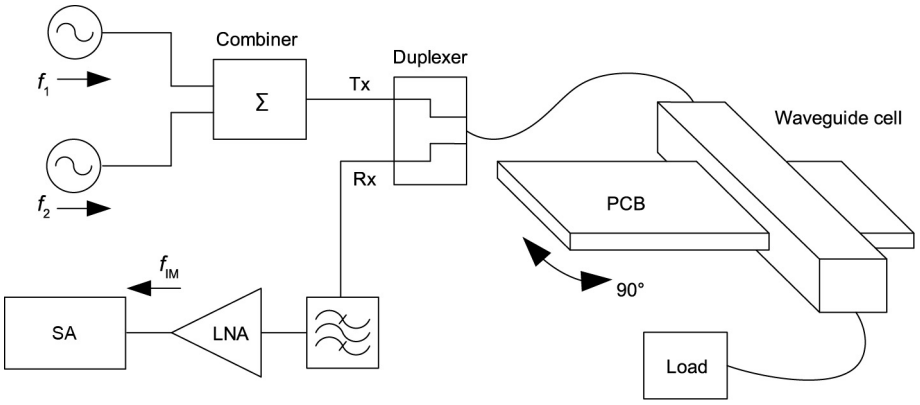

Fig. 8. Block diagram of a localization method with a waveguide cell [59]. PCB: printed circuit board.

existing in the space may also be received by the DUT. All these signals will interfere with the measurement of PIM, resulting in large test errors. The PIM values measured in or outside the chamber may differ by tens of decibel. Thus, to carry out accurate and reliable PIM measurement, an anechoic chamber is needed for confining the testing space and for shielding the external noise as well as for minimizing the internal reflection from the chamber walls.

However, there are also PIM sources inside the chamber; the main sources of PIM are the non-linearity in the reflective wave from the absorbing material and the shielding enclosures [60,61]. As shown in Fig. 9 [60], an example can be considered based on the antenna reflection test where f_1 and f_2 are the frequencies of two working signals. S_{IM_Ai} is the reverse PIM of the antenna under test (AUT); S_{IM_Ar} is also from the AUT but it is generated by the reflected signals S'_{f_1} and S'_{f_2} (S'_{f_1} and S'_{f_2} are the echo signals of f_1 and f_2 reflected by the chamber); S'_{IM_Ai} is the echo signal of S_{IM_Ai} reflected by the chamber; S_{IM_AM} and S_{IM_SE} are the PIM from the absorbers and chamber walls, respectively; S_{IM_EX} refers to the signal from the outside of the test chamber; and S_{IM_SYS} represents the total PIM noise of the test instrument.

Most of these signals can be estimated by indicators such as reflection level and shielding effectiveness of chamber; however, the magnitude of S_{IM_AM} and S_{IM_SE} is unknown. According to previous reports, the measurement error caused by no specially designed shielding enclosures and absorbing materials may exceed 10 dB [60,61]. The traditional method aimed at reducing these PIM signals is to build a huge chamber. Then, the PIM level could be reduced by the large path loss. Of course, larger size means higher cost and more space, and it is difficult to move or transport. Moreover, some size requirements may not be fulfilled by general factory building. These problems make the traditional PIM test chamber very inconvenient and expensive. A small-sized chamber will be easier to assemble and relocate, with low cost and high efficiency.

The key to miniaturizing the PIM chamber is to design low-PIM absorbers and shielding enclosures. People proved that if the absorbers and the shielding enclosures do not produce PIM, the size of the chamber becomes irrelevant [60]. At the same time, it was also proposed a usable low-PIM absorbing material and shielding structure in the same Ref. [60].

Both PIM performance and shielding effectiveness must be taken into consideration when designing and manufacturing shielding enclosures. As shown in Fig. 10 [60], the key for an effective design is to avoid large-area metal–metal contacts; whereas any unavoidable large-area contacts should be moved out of the chamber by re-designing the joint structure. The metal plates to be used should be non-ferromagnetic and have a flat solid structure rather than made by a wire mesh fabric that may generate PIM. The multi-layer metal plate structure and the use of lossy material can achieve a good shielding effect at the metal–metal joints.

Absorbing materials need to have good absorption performances while keeping low PIM. The good absorption property reduces the reflection level of the chamber and, at the same time, can attenuate the signal reaching the shielding enclosures, which can inherently reduce the PIM level of S_{IM_SE}.

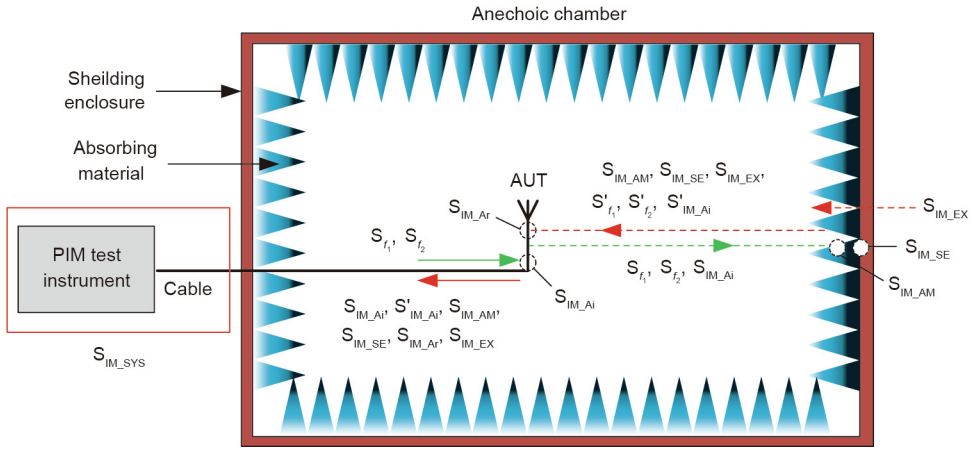

Fig. 9. PIM signals in test chamber [60]. S_{IM_SYS}: the total PIM noise of the test instrument; S'_{f_1}, S'_{f_2}: the echo signals of f_1 and f_2 reflected by the chamber; S_{IM_AM}, S_{IM_SE}: the PIM from the absorbers and chamber walls, respectively; S_{IM_EX}: the signal from the outside of the test chamber; AUT: antenna under test; S_{IM_Ai}: the reverse PIM of the AUT; S_{IM_Ar}: from AUT but generated by S'_{f_1} and S'_{f_2}; S'_{IM_Ai}: the echo signal of S_{IM_Ai} reflected by the chamber.

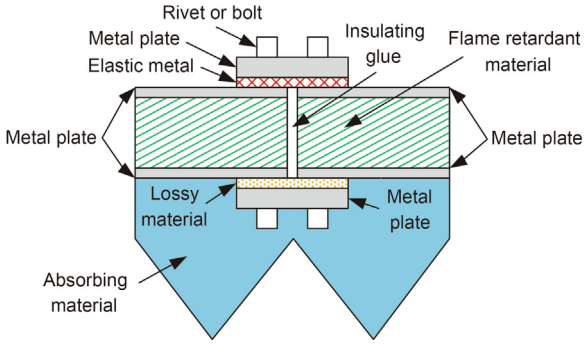

Fig. 10. Splicing structure of shielding enclosure [60].

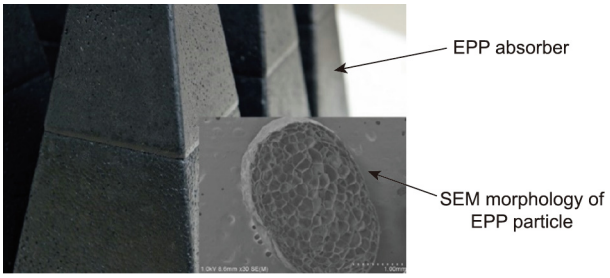

Fig. 11. EPP absorber and SEM morphology of EPP particle [60]. SEM: scanning electron microscope.

Most anechoic chambers employ pyramid absorbers made of polyurethane (PU) foam, carbon particles, or graphite powder. The process flow is simple, mainly including soaking and drying the carbon powder mixture. This kind of process is relatively rough, and there may be shortcomings such as material unevenness and unstable performance. For PIM, there could be loose carbon particle contact in the materials manufactured by this process, which will lead to the appearance of PIM products [1].

Expanded polypropylene (EPP) has begun to be used as an absorbing material for anechoic chambers in recent years [71]. The absorbent in this material uses nano-scale carbon black (CB), which is finer than traditional micron-scale graphite particles in the PU-based absorber. During the molding process, the nano-scale CB particles could be in full contact. Thus, it has uniformly distributed nanoparticles and is stable in dielectric properties. Fig. 11 [60] shows the EPP absorber and its morphology under a scanning electron microscope (SEM). It can be seen that it is difficult to see individual CB particles even in the SEM image, which may be the responsibility of the PIM noise. Therefore, the EPP absorber is not only superior to traditional PU materials in absorbing performance, but also has a low PIM level since the particles are within the nanometer scale and are uniformly distributed. Experiments in Ref. [60] show that, compared to traditional sponge absorbing materials, EPP has excellent performance and almost no PIM products are generated.

The relevant aspects discussed above about the design of PIM test chamber suggests that future standards should incorporate the design requirements of the PIM test chamber.

4.4. Challenge and solution to evaluate the performance of PIM test chamber

Once designed and manufactured by taking into account the aspects discussed above, the performances of the PIM test chamber should be accordingly evaluated. This process can be divided into two parts: the evaluation of the components and of the entire chamber.

The component evaluation is of great significance to the designer and manufacturer of anechoic chamber. It can ensure that the components used will not cause PIM interference. The main objects of the evaluation are the absorbing materials and the shielding enclosures. The evaluation index is the PIM performance of each component. The evaluation method can use the PIM measurement method of non-ported devices (reflector, antenna support, etc.) according to the schematic diagram displayed in Fig. 12 [72,73]. Since the DUT is a non-ported component and does not generate signals, two single-frequency signals can be transmitted through two transmitting antennas. When the electromagnetic waves illuminate the DUT, a PIM signal will be generated. Then it can be received by the receiving probe. In Fig. 12, the transmitting antenna and the receiving antenna can be shared [72,73]. But this requires the probe to have a very low PIM level, otherwise it will cause large errors in the measurement results.

The overall evaluation is used for the final acceptance of the PIM test chamber. As mentioned in Section 1, the residual PIM of the chamber is related to the gain of the DUT. Therefore, in theory, a low-PIM antenna with a sufficiently high gain should be used to detect the PIM noise of the chamber. However, the structure of a high-gain antenna is relatively complex, with more connection

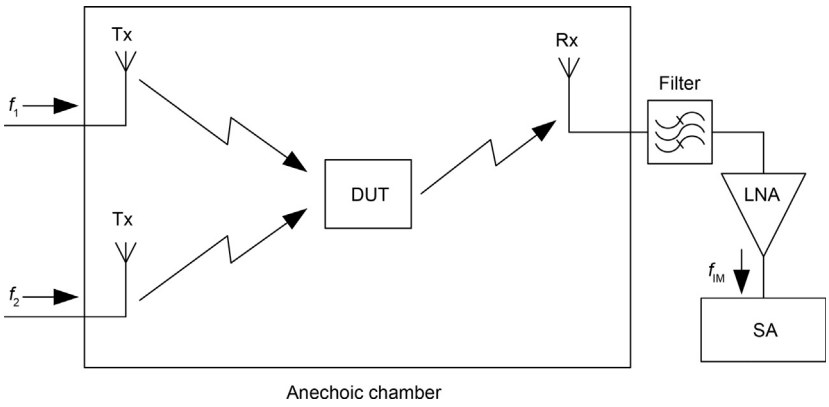

Fig. 12. Radiation test method of non-ported components.

points, soldering points, and nonlinear devices. Therefore, it is difficult to achieve very low PIM levels. In addition, high-gain antennas have large apertures and narrow beams. It is very difficult to rotate a large antenna (such as a base station antenna) to scan it within the chamber for a comprehensive analysis. A method of measuring the chamber by using a medium-gain low-PIM antenna is proposed in Ref. [61]. The power received from the chamber wall can be increased by shortening the distance from the maximum gain direction of the antenna to the chamber wall. Then, the medium-gain antenna can achieve an effect similar to the high-gain antenna. The medium-gain antenna can be realized with only a single unit. It is easy to achieve a low PIM compared to a high-gain antenna, and it is usually smaller in size, which has the advantage of better flexibility to be moved or rotated. Thus, the medium-gain antenna is more convenient in terms of design and applicability. The method has been verified by experiments and its feasibility has been proved. However, more rigorous analysis and engineering practices for defining standard guidelines are still needed.

5. Summary

Measurement is deemed to be the most effective method to study PIM interference. In this review, the challenges and solutions faced by PIM measurements are comprehensively introduced. The current PIM measurement standards provide basic measurement methods such as transmission, reflection, and radiation methods. However, some key issues in PIM measurements are not raised enough attention such as the design of the PIM tester, the identification method of the PIM source location, the design method of compact and cheaper PIM chambers, and the technique for evaluating the overall performances of the PIM chamber. The feed-forward cancellation technology can effectively reduce the PIM interference of the system and greatly improve the dynamic range of the PIM tester [14]. The Acoustic vibration method proposed in Ref. [19] can effectively locate the PIM source, and it is a method with more practical values among other positioning methods currently used. A variety of location methods have been proposed, such as near-field scanning method, acoustic vibration method, and *k*-space multicarrier signal method, as reviewed and summarized in this paper, in order to locate PIM sources in different environments and systems [46–59]. A design method for achieving a low-PIM chamber was proposed in Ref. [60], and it was proved that the size of the chamber becomes insignificant in PIM measurements provided there is no PIM source from the chamber. The chamber design based on specific assembly process and specifically developed absorbing materials can be used as a guide for designing a compact PIM chamber. A PIM anechoic chamber evaluation method is proposed in Ref. [61], which can use a medium-gain antenna to evaluate the interference of a high-gain antenna in the anechoic chamber. The aspects and techniques discussed in this paper are of great significance for solving PIM problems, to effectively locate the source of PIM and to build a low-cost compact environment with extremely low residual PIM. This paper may set the base for additional and more specific work concerning the even more demanding PIM test requirements of satellites and 5G base stations.

With the development of wireless communication technology, the problem of the PIM involves complex multi-physics conditions, multi-modulation modes, and overlapping channels, thus it may become a hot research topic to be further expanded and deeply investigated for achieving feasible solutions. In this context, instruments able to identify and evaluate the amount of PIM within a wide bandwidth and dynamic range may be required in the future. Moreover, compared with the current diversified location methods, the future PIM source location methods should be accurately developed and then standardized, in order to be applied to a larger variety of devices with common outcomes. In the case of PIM test chambers, standards should also be established, as part of the future development of PIM analysis methodologies and instruments. Finally, PIM is susceptible to environmental interference (temperature changes or environmental stress, etc.), and high-sensitivity real-time monitoring equipment may be required in some cases.

Compliance with ethics guidelines

Zhanghua Cai, Lie Liu, Francesco de Paulis, and Yihong Qi declare that they have no conflict of interest or financial conflicts to disclose.

References

[1] Lui PL. Passive intermodulation interference in communication systems. Electr Commun Eng J 1990;2(3):109–18.
[2] Sanford J. Passive intermodulation considerations in antenna design. In: Proceedings of IEEE Antennas and Propagation Society International Symposium; 1993 Jun 28–Jul 2; Ann Arbor, MI, USA. IEEE; 1993. p. 1651–4.
[3] TR 37.808: Passive intermodulation (PIM) handling for base stations (BS). 3GPP standard. France: 3GPP; 2013.
[4] Butler R. PIM testing: advanced wireless services emphasize the need for better PIM control. Report. Soochow: CommScope; 2017.
[5] Hienonen S. Studies on microwave antennas: passive intermodulation distortion in antenna structures and design of microstrip antenna elements [dissertation]. Helsinki: Helsinki University of Technology; 2005.
[6] Wilkerson JR. Passive intermodulation distortion in radio frequency communication systems [dissertation]. Raleigh: North Carolina State University; 2010.
[7] Simmons JG. Generalized formula for the electric tunnel effect between similar electrodes separated by a thin insulating film. J Appl Phys 1963;34(6):1793–803.

[8] Higa WH. Spurious signals generated by electron tunneling on large reflector antennas. Proc IEEE 1975;63(2):306–13.
[9] Bond C, Guenzer C, Carosella C. Intermodulation generation by electron tunneling through aluminum–oxide films. Proc IEEE 1979;67(12):1643–52.
[10] Sorolla E, Anza S, Gimeno B, Perez AMP, Vicente C, Gil J, et al. An analytical model to evaluate the radiated power spectrum of a multipactor discharge in a parallel-plate region. IEEE Trans Elect Devices 2008;55(8):2252–8.
[11] Wen H, Yang H, Kuang H, Qin X, Cai G. Global threshold prediction of multicarrier multipactor with time distribution and material coefficients. IEEE Trans Electromagn Compat 2017;60(5):1163–70.
[12] You JW, Wang HG, Zhang JF, Tan SR, Cui TJ. Accurate numerical analysis of nonlinearities caused by multipactor in microwave devices. IEEE Microw Wirel Compon Lett 2014;24(11):730–2.
[13] Wilkerson JR, Gard KG, Schuchinsky AG, Steer MB. Electro–thermal theory of intermodulation distortion in lossy microwave components. IEEE Trans Microw Theory Tech 2008;56(12):2717–25.
[14] Chen X, Wang L, Pommerenke D, Yu M. Passive Intermodulation on coaxial connector under electro–thermal–mechanical multiphysics. IEEE Trans Microw Theory Tech 2021;70(1):169–77.
[15] Ansuinelli P, Schuchinsky AG, Frezza F, Steer MB. Passive intermodulation due to conductor surface roughness. IEEE Trans Microw Theory Tech 2018;66(2):688–99.
[16] Zhao X, He Y, Ye M, Gao F, Peng W, Li Y, et al. Analytic passive intermodulation model for flange connection based on metallic contact nonlinearity approximation. IEEE Trans Microw Theory Tech 2017;65(7):2279–87.
[17] Vicente C, Hartnagel H. Passive-intermodulation analysis between rough rectangular waveguide flanges. IEEE Trans Microw Theory Tech 2005;53(8):2515–25.
[18] Bahrami M, Culham J, Yovanovich M. Modeling thermal contact resistance: a scale analysis approach. J Heat Transf 2004;126(6):896–905.
[19] Bailey GC, Ehrlich AC. A study of RF nonlinearities in nickel. J Appl Phys 1979;50(1):453–61.
[20] Bertotti G. General properties of power losses in soft ferromagnetic materials. IEEE Trans Magn 2002;24(1):621–30.
[21] Chen X, He Y. Reconfigurable passive intermodulation behavior on nickel-coated cell array. IEEE Trans Electromagn Compat 2017;59(4):1027–34.
[22] Henrie J, Christianson AJ, Chappell WJ. Linear–nonlinear interaction and passive intermodulation distortion. IEEE Trans Microw Theory Tech 2010;58(5):1230–7.
[23] Henrie J, Christianson A, Chappell WJ. Engineered passive nonlinearities for broadband passive intermodulation distortion mitigation. IEEE Microw Wirel Compon Lett 2009;19(10):614–6.
[24] Guo H, Yao Y, Xie Y. Evaluation of passive intermodulation from multiple connectors with generalized network method. IEEE Microw Wirel Compon Lett 2021;31(3):312–5.
[25] Jin Q, Gao J, Flowers GT, Wu Y, Xie G. Modeling of passive intermodulation with electrical contacts in coaxial connectors. IEEE Trans Microw Theory Tech 2018;66(9):4007–16.
[26] Jin Q, Gao J, Flowers GT, Wu Y, Xie G, Bi L. Modeling of passive intermodulation in connectors with coating material and iron content in base brass. IEEE Trans Microw Theory Tech 2019;67(4):1346–56.
[27] Shitvov AP, Zelenchuk DE, Schuchinsky AG, Fusco VF. Passive intermodulation generation on printed lines: near-field probing and observations. IEEE Trans Microw Theory Tech 2008;56(12):3121–8.
[28] Shitvov AP, Olsson T, Banna BE, Zelenchuk DE, Schuchinsky AG. Effects of geometrical discontinuities on distributed passive intermodulation in printed lines. IEEE Trans Microw Theory Tech 2010;58(2):356–62.
[29] Rocas E, Collado C, Orloff ND, Mateu J, Padilla A, O'Callaghan JM, et al. Passive intermodulation due to self-heating in printed transmission lines. IEEE Trans Microw Theory Tech 2011;59(2):311–22.
[30] Zelenchuk DE, Shitvov AP, Schuchinsky AG, Fusco VF. Passive intermodulation in finite lengths of printed microstrip lines. IEEE Trans Microw Theory Tech 2008;56(11):2426–34.
[31] Kozlov DS, Shitvov AP, Schuchinsky AG, Steer MB. Passive intermodulation of analog and digital signals on transmission lines with distributed nonlinearities: modelling and characterization. IEEE Trans Microw Theory Tech 2016;64(5):1383–95.
[32] Vicente C, Wolk D, Hartnagel HL, Gimeno B, Boria VE, Raboso D. Experimental analysis of passive intermodulation at waveguide flange bolted connections. IEEE Trans Microw Theory Tech 2007;55(5):1018–28.
[33] Liu Y, Mao YR, Xie YJ, Tian ZH. Evaluation of passive intermodulation using full-wave frequency-domain method with nonlinear circuit model. IEEE Trans Veh Technol 2016;65(7):5754–7.
[34] Mao YR, Liu Y, Xie YJ, Tian ZH. Simulation of electromagnetic performance on mesh reflector antennas: three-dimensional mesh structures with lumped boundary conditions. IEEE Trans Antennas Propag 2015;63(10):4599–603.
[35] Figueiredo R, Carvalho NB, Piacibello A, Camarchia V. Nonlinear dynamic RF system characterization: envelope intermodulation distortion profiles—a noise power ratio-based approach. IEEE Trans Microw Theory Tech 2021;69(9):4256–71.
[36] Chen X, Sun D, Cui W, He Y. A folded contactless waveguide flange for low passive-intermodulation applications. IEEE Microw Wirel Compon Lett 2018;28(10):864–6.
[37] Henrie J, Christianson A, Chappell WJ. Cancellation of passive intermodulation distortion in microwave networks. In: Proceedings of 2008 38th European Microwave Conference; 2008 Oct 27–31; Amsterdam, Netherlands. IEEE; 2008. p. 1153–6.
[38] Waheed MZ, Korpi D, Anttila L, Kiayani A, Kosunen M, Stadius K, et al. Passive intermodulation in simultaneous transmit-receive systems: modeling and digital cancellation methods. IEEE Trans Microw Theory Tech 2020;68(9):3633–52.
[39] Jin Q, Gao J, Huang H, Bi L. Mitigation methods for passive intermodulation distortion in circuit systems using signal compensation. IEEE Microw Wirel Compon Lett 2020;30(2):205–8.
[40] Miao X, Tian L. Digital cancellation scheme and hardware implementation for high-order passive intermodulation interference based on hammerstein model. China Commun 2019;16(9):165–76.
[41] Keehr EA, Hajimiri A. Successive regeneration and adaptive cancellation of higher order intermodulation products in RF receivers. IEEE Trans Microw Theory Tech 2011;59(5):1379–96.
[42] IEC62037: Passive RF and Microw devices intermodulation level measurement. International standard. Geneva: International Electrotechnical Commission; 2021.
[43] Wilkerson JR, Gard KG, Steer MB. Automated broadband high-dynamic-range nonlinear distortion measurement system. IEEE Trans Microw Theory Tech 2010;58(5):1273–82.
[44] Waheed MZ, Campo PP, Korpi D, Kiayani A, Anttila L, Valkama M. Digital cancellation of passive intermodulation in FDD transceivers. In: Proceedings of 2018 52nd Asilomar Conference on Signals, Systems, and Computers; 2018 Oct 28–31; Pacific Grove, CA, USA. IEEE; 2018. p. 1375–81.
[45] Wetherington JM, Steer MB. Robust analog canceller for high-dynamic-range radio frequency measurement. IEEE Trans Microw Theory Tech 2012;60(6):1709–19.
[46] Range to fault (RTF) [Internet]. Spokane Valley: Kaelus; c2020 [cited 2021 Aug 30]. Available from: https://www.kaelus.com/en/test-measurement-solutions/portable-pim-testing/range-to-fault-(rtf)-en.
[47] PIM rack analyzer [Internet]. Fridolfing: Rosenberger; c2018 [cited 2021 Aug 30]. Available from: https://www.rosenberger.com/product/pim-rack-analyzer/.
[48] anritsu.com [Internet]. Kanagawa: Anritsu; c2022 [cited 2021 Aug 30]. Available from: https://www.anritsu.com/en-us/test-measurement/support/downloads?model=MW82119B.
[49] Hienonen S, Vainikainen P, Raisanen AV. Sensitivity measurements of a passive intermodulation near-field scanner. IEEE Antennas Propag Mag 2003;45(4):124–9.
[50] Hienonen S, Golikov V, Vainikainen P, Raisanen AV. Near-field scanner for the detection of passive intermodulation sources in base station antennas. IEEE Trans Electromagn Compat 2004;46(4):661–7.
[51] Shitvov AP, Zelenchuk DD, Schuchinsky AG, Fusco VF, Buchanan N. Mapping of passive intermodulation products on microstrip lines. In: Proceedings of 2008 IEEE MTT-S International Microwave Symposium Digest; 2008 Jun 15–20; Atlanta, GA, USA. IEEE; 2008. p. 1573–6.
[52] Oonishi K, Kuga N. A consideration of sensitivity of non-contact PIM measurement using a coaxial probe. In: Proceedings of 2008 Asia-Pacific Microwave Conference; 2008 Dec 16–20; Hong Kong, China. IEEE; 2008. p. 1–4.
[53] Yang S, Wu W, Xu S, Zhang YJ, Stutts D, Pommerenke DJ. A passive intermodulation source identification measurement system using a vibration modulation method. IEEE Trans Electromagn Compat 2017;59(6):1677–84.
[54] Zhang M, Zheng C, Wang X, Chen X, Cui W, Li J, et al. Localization of passive intermodulation based on the concept of *k*-space multicarrier signal. IEEE Trans Microw Theory Tech 2017;65(12):4997–5008.
[55] Aspden PL, Anderson AP, Bennett JC. Microwave holographic imaging of intermodulation product sources applied to reflector antennas. In: Proceedings of 1989 Sixth International Conference on Antennas and Propagation; 1989 Apr 4–7; Coventry, UK. IET; 1989. p. 463–7.
[56] Aspden PL, Anderson AP. Identification of passive intermodulation product generation on microwave reflecting surfaces. IEE Proc H 1992;139(4):337–42.
[57] Aspden PL, Anderson AP, Bennett JC. Evaluation of the intermodulation product performance of reflector antennas and related structures by microwave imaging. In: Proceedings of 1989 19th European Microwave Conference; 1989 Sep 4–7; London, UK. IEEE; 1989. p. 853–8.
[58] Yong S, Yang S, Zhang L, Chen X, Pommerenke DJ, Khilkevich V. Passive intermodulation source localization based on emission source microscopy. IEEE Trans Electromagn Compat 2020;62(1):266–71.
[59] Chen X, An L, Yu M, Pommerenke DJ. Waveguide cell with water filling for passive intermodulation localization on planar circuits. IEEE Microw Wirel Compon Lett 2021;31(11):1247–50.
[60] Cai Z, Zhou Y, Liu L, Qi Y, Yu W, Fan J, et al. Small anechoic chamber design method for on-line and on-site passive intermodulation measurement. IEEE Trans Instrum Meas 2020;69(6):3377–87.
[61] Cai Z, Zhou Y, Liu L, Paulis FD, Qi Y, Orlandi A. A method for measuring the maximum measurable gain of a passive intermodulation chamber. Electronics 2021;10(7):770.
[62] Denisowski P. Understanding PIM. Report. Munich: Rohde&Schwarz; 2019 Nov.
[63] ITU-R SM.1446: Definition and measurement of intermodulation products in transmitter using frequency, phase, or complex modulation techniques. International standard. Geneva: Radiocommunication Sector of ITU; 2011.
[64] Kim JT, Cho IK, Jeong MY, Choy TG. Effects of external PIM sources on antenna PIM measurements. ETRI J 2002;24(6):435–42.

[65] Shi C, Sánchez-Sinencio E. On-chip two-tone synthesizer based on a mixing-FIR architecture. IEEE J Solid-State Circuits 2017;52(8):2105–16.
[66] Yoshida S, Kuga N. A planar band rejection filter composed of slit-loaded side-coupled filter for 3rd-order PIM measurement. In: Proceedings of 2009 Asia Pacific Microwave Conference; 2009 Dec 7–10; Singapore. IEEE; 2009. p. 2613–6.
[67] Smacchia D, Soto P, Guglielmi M, Morro JV, Boria V, Raboso D. Implementation of waveguide terminations with low-passive intermodulation for conducted test beds in backward configuration. IEEE Microw Wirel Compon Lett 2019;29(10):659–61.
[68] Maheshwari P, Kajbaf H, Khilkevich VV, Pommerenke D. Emission source microscopy technique for EMI source localization. IEEE Trans Electromagn Compat 2016;58(3):729–37.
[69] Zhang L, Khilkevich VV, Jiao X, Li X, Toor S, Bhobe AU, et al. Sparse emission source microscopy for rapid emission source imaging. IEEE Trans Electromagn Compat 2017;59(2):729–38.
[70] Sørensen M, Kajbaf H, Khilkevich VV, Zhang L, Pommerenke D. Analysis of the effect on image quality of different scanning point selection methods in sparse ESM. IEEE Trans Electromagn Compat 2019;61(6):1823–31.
[71] Zhang Y, Luo Q, Zhu Y, Liu L. Development of conductive expended polypropylene rigid foam for OTA test chamber. Saf EMC 2017;16:59–62.
[72] Bolli P, Selleri S, Pelosi G. Passive intermodulation on large reflector antennas. IEEE Antennas Propag Mag 2002;44(5):13–20.
[73] Smacchia D, Soto P, Boria VE, Guglielmi M, Carceller C, Ruiz Garnica J, et al. Advanced compact setups for passive intermodulation measurements of satellite hardware. IEEE Trans Microw Theory Tech 2018;66(2):700–10.